Mutual Coupling Reduction of a Dual-Band Antenna Array Using Dual-Frequency Metamaterial Structure

Shengyuan Luo [1], Yingsong Li [1,2,*], Yinfeng Xia [1], Guohui Yang [3], Laijun Sun [4], and Lei Zhao [5]

[1] College of Information and Communication Engineering
Harbin Engineering University, Harbin, Heilongjiang 150001, China

[2] National Space Science Center, Chinese Academy of Sciences, Beijing 100190, China
*liyingsong@ieee.org

[3] School of Electronics and Information Engineering, Harbin Institute of Technology, Harbin 150001, China

[4] College of Electronic Engineering, Heilongjiang University, Harbin, 150080

[5] Center for Computational Science and Engineering, School of Mathematics and Statistics
Jiangsu Normal University, Xuzhou, China

Abstract ─ Dual-band antenna is an enabling component for wireless local area network (WLAN) communication systems. One of the challenges for improving the communication quality in dual-band multiple-input multiple-output (MIMO) system is to develop low coupling MIMO antenna array with compact size. In this paper, an isolation enhanced two-element MIMO antenna array with dual-frequency decoupling structure is proposed for operating at the upper and lower WLAN bands. The proposed dual-frequency decoupling structure is realized by an array of two columns of metamaterial structures with unique electromagnetic resonance characteristic. The property of the designed metamaterial array is analyzed and integrated between the elements of a two-element patch antenna array to reduce the mutual coupling. The performance of the dual-frequency patch antenna array is verified by the simulation and measurement, respectively. The experimental results show that the proposed dual-frequency MIMO antenna array has an isolation enhancement about 15dB at 2.4GHz and 9dB at 5.25GHz, respectively. Moreover, the proposed dual-band MIMO antenna has a smaller size and good directional radiation patterns, making it promising for WLAN applications.

Index Terms ─ Dual-band, MIMO, mutual decoupling, WLAN.

I. INTRODUCTION

With the development of wireless communication technologies, the antenna design carts an increasing demand since it is required to transmit and receive the electromagnetic signals [1]. In order to improve the communication quality, multiple-input multiple-output (MIMO) technique has been applied for wireless communications and it is also considered as a technique for construct massive MIMO system in next generation communication systems [2]. Furthermore, the wireless local area network (WLAN) has been used for a long time, which needs to operate at dual frequency mode to incorporate 802.11 a/b/g/n/ac/ax standards. The antennas mentioned in [1-2] is printed on low cost substrate to utilize the characteristics like light weight, small volume and easy fabrication.

As for MIMO WLAN communication system, the design of the dual-band MIMO antenna has been applied to practical applications. So far, many methods have been exploited to design MIMO multi-band antennas that contain the WLAN band [3-11]. For the small dual-band antenna designs, the most mature technologies to obtain multi-band characteristics includes exciting multiple-mode [12-14] and engraving a groove on the micros-trip patch[15-16], using multilayer structure or multi-stubs to form resonators and use multiple patches technology [17-20].

For the small dual-band antenna designs, the most mature technologies to obtain multi-band characteristics includes exciting multiple-mode and engraving a groove on the micros-trip patch [15-16], using multilayer structure and multiple patches technology [17-19]. The dual-mode excitation technology may have two narrow operating bands for WLAN communication, but it has

Submitted On: November 22, 2018
Accepted On: December 24, 2018

advantages to provide multiple bands without changing the structure of the patch antenna and the radiation patterns.

On the other hand, the channel capacity and the throughput of the MIMO communication system might be reduced when the received signals at multiple receiving antennas are correlated [2]. Therefore, the mutual coupling (MC) from the adjacent antenna elements in the MIMO antenna array may degrade the efficiency, correlation and eventually deteriorate the communication quality of the entire MIMO system [20-21]. Some of the researchers paid much efforts to optimize the precoding strategies on both the receiver and transmitter sides to reduce the MC to design a compact large-scale MIMO system [22-23]. Recently, the compact device will limit the size of the components, which makes the MIMO antenna array smaller and smaller. Thus, the MC issue in the compact MIMO antenna array is an inevitable factor that seriously affects the MIMO antenna performance in small terminals. How to reduce the MC in the MIMO array becomes to be a hot topic which attracts more and more attention in recent years [20-23]. Especially for the compact dual-band MIMO antenna array that is used for dual-band WLAN communication and the MC problem becomes a key issue that should be resolved simultaneously at the lower and upper WLAN bands.

In general, the MC is serious when the antenna elements are placed less than half-wavelength, which will deteriorate the radiating performance and reduce the channel capacity. Thus, it is very useful to design decoupling structure to reduce the MC between the antenna elements [24]. Currently, many amazing mutual decoupling structures such as decoupling network, defected ground structure (DGS), electromagnetic band gap (EBG) and metamaterial are used in MIMO antenna array [25-38]. For the decoupling network, the typical decoupling structure is to use a stub in the ground plane of a MIMO antenna array, such as the T-shaped stub [25-27], which will affect the radiation patterns of the antenna array. Recently, an improved decoupling network has been proposed in [28]. It demonstrated that the coupled decoupling structure can reduce the MC over two bands, which is still realized based on stub technologies. Also, the periodic DGS has been developed to improve the isolation in the MIMO antenna array [29-31]. However, the DGS destroys the integrity of the ground plane, which may leak electromagnetic wave and affect the radiation patterns. Another effective method to enhance the isolation of antenna array is to use the EBG structure in antenna array [32-36]. Unlike the previous decoupling technologies, the EBG structure has been introduced into the middle of the antenna elements, and it can prohibit the microwave propagation between antenna elements because of its high impendence property. The resonance of the EBG is caused by the inductance of the EBG cell structure itself and the capacitance between the EBG units.

In the past decades, the metamaterial decoupling techniques have attracted more attention because of its unique property, and it can perform high impendence, negative permittivity and negative permeability, negative refractive index. Moreover, the metamaterial decoupling has some advantages such as small size, easy fabrication. The resonance of the metamaterial is caused by the capacitance and inductance of the metamaterial cell itself. Therefore, although the structure of the EBG and metamaterial is similar, the basic resonance principle is different. For the decoupling network, DGS, EBGs, they are not easy to obtain a dual-band property because they need to redesign the entire structures. But, it is easy to achieve a dual-band negative permittivity by integrating two conventional SRRs into the same metamaterial structure, and the designed dual-band meta-material has been used for reducing the MC between the MIMO antenna elements by adjusting the dimensions of the two SRRs. [37-39]. However, these MIMO antennas only have one band by using the metamaterial decoupling structure. Currently, the dual-band antenna array becomes more and more useful because of its potential applications in modern wireless communication systems. Thus, how to reduce the MC between the dual-band antenna array elements becomes an urgent issue.

Based on the advantages of the planar metamaterial, a high isolation dual-band MIMO antenna array is proposed by using dual-frequency metamaterial structure operating at WLAN bands. Compared to existing technologies, our proposed method has the following unique features:

(1) The designed MIMO antenna array with high isolation covers the lower and upper WLAN bands.

(2) Dual-frequency metamaterial is used to reduce the MC of the dual-band WLAN MIMO antenna array.

(3) The designed planar dual-band metamaterial can be independently adjusted to achieve a good match with the desired dual-band MIMO antenna array without affecting the performance of the MIMO array.

II. DESIGN OF THE PROPOSED DUAL-BAND WLAN MIMO ARRAY

A. Dual-band microstrip antenna

According to the rectangular microstrip antenna theory and the multiple mode excitation scheme, a dual-band microstrip antenna is developed with only one feeding, which is shown in Fig. 1. The proposed antenna has a simple rectangle patch printed on a FR4 substrate with a relative permittivity of 4.4 and a loss tangent of 0.02, and there is a ground plane set at the bottom of the FR4. Then, a coaxial probe feeding is used to excite the two modes. The longer side excites the TM_{10} mode to generate the lower frequency, while the short side excites the TM_{01} mode to give the upper band.

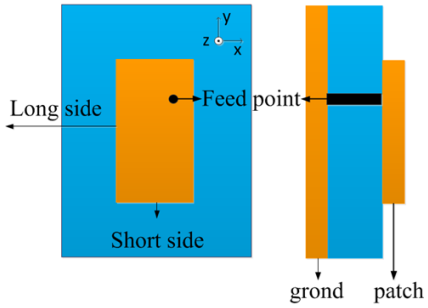

Fig. 1. The mechanism of dual-band patch antenna.

B. Principle of dual-band metamaterial

The schematic of a metamaterial comes from the resonance of the inductance in metal patch and the capacitance in the split ring resonator (SRR). For metamaterial structure, the resonance is caused by the inductance and capacitance of the SRR structure, while the dual-band metamaterial proposed in this paper is realized by the inductance and the two different capacitances. When two different SRRs are connected by a metal strip and placed on the same substrate, the inductance significantly increases while the capacitance does not change. Thus, two resonant frequencies are obtained. Comparing with the original single-band SRR, the proposed integrated SRR (ISRR) structure shown in Fig. 2 (a) has a more complicated design procedure. However, the ISRR can provide more bands, and the size is greatly reduced. Additionally, each band can be independently adjusted to match with the desired resonant frequency. Based on the theory of the metamaterial, a metamaterial based on the ISRR is designed and given in Fig. 2 (b). Figure 2 (c) shows the 3-demesion structure of the proposed metamaterial cell. Since the ISRR has an adjustable band, the proposed metamaterial cell can be flexibly designed to meet the desired resonance band requirements. To understand the performance of the proposed metamaterial cell, the perfect H, and perfect E boundaries, and wave port are used to analyze its characteristics.

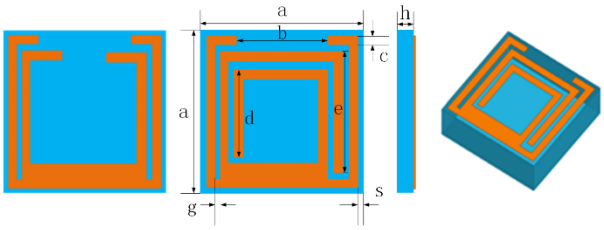

Fig. 2. Geometry of DBMC: (a) SRR structure, (b) proposed metamaterial cell, and (c) the 3-D structure of the DBMC.

Figure 3 presents the equivalent circuit of the proposed dual-band metamaterial cell. The split size controls the C_1, the overall size of the outer SRR controls the L_1, and the R_1 is the resistance of the outer SRR itself. C_2 is the capacitance between the two branches of the inner SRR. The R_2 and R_3 are the resistances of two branches of the inner SRR. Correspondingly, the L_2 and L_3 are the inductance of two branches of the inner SRR. Figure 4 presents the simulation model of the proposed dual-band metamaterial cell (DBMC), which is created in the HFSS. In fact, the gap between the SRRs and the length of the SRRs control the metamaterial property, which can be obtained by the numerical analysis. Figure 5 gives the transmission coefficient (S_{21}) and reflection coefficient (S_{11}) of the DBMC with different parameters. When b increases from 2mm to 4mm shown in Fig. 5 (a), the bandwidth of the center frequency of the upper band is changed while the bandwidth for the lower band remains same.

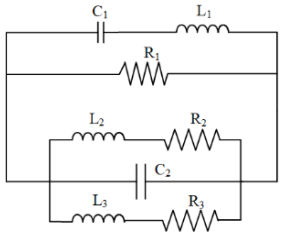

Fig. 3. The equivalent circuit of the proposed DBMC.

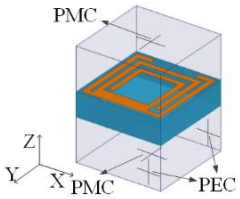

Fig. 4. Simulation model of the proposed dual-band metamaterial cell.

Figure 5 (b) presents the effects of various b on the phase difference of S_{11} and S_{21}. It is found that the phase at the upper band changes quickly with different parameter b. Then, the S-parameter method is utilized to retrieve the dielectric constant of designed DBMC, and the results are described in Fig. 5 (c). The negative permeability characteristics of the upper band move to higher frequency with the increment of parameter b. Then, the parameter e that gives important effects on the performance of the proposed DBMC is investigated in detail. Figure 6 (a) illustrates magnitude difference of S_{11} and S_{21} with different length e ranging from 2mm to 4mm of the ISRR. The frequency of the lower band

becomes to be smaller with an increasing e due to the coupling between the modified SRRs. The phase difference for different e is given in Fig. 6 (b). It is observed that the phase for both the upper band and lower band changes so fast with different parameter e. Then, the S-parameter method is considered to retrieve the dielectric constant of designed DBMC, and the results are presented in Fig. 6 (c). The negative permeability characteristics of the lower band shifts very quickly with various e.

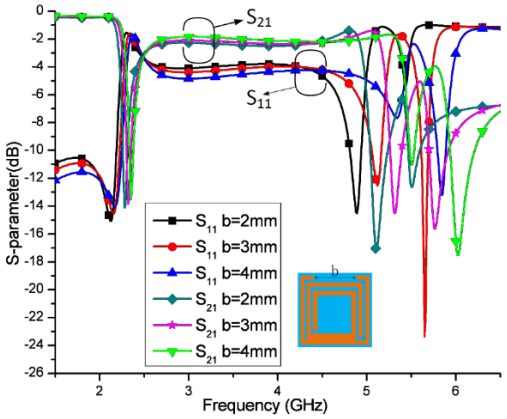

(a) Magnitude difference of the DBMC

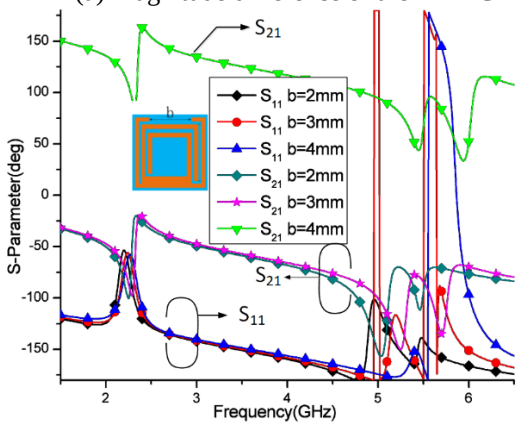

(b) Phase difference of the DBMC

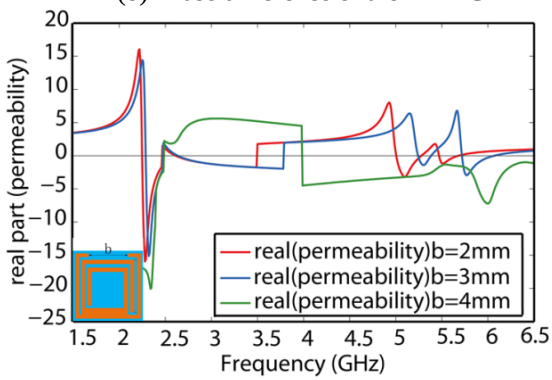

(c) Negative permittivity characteristics of the DBMC

Fig. 5. Performance of the proposed DBMC with different b dual-band MIMO antenna array elements.

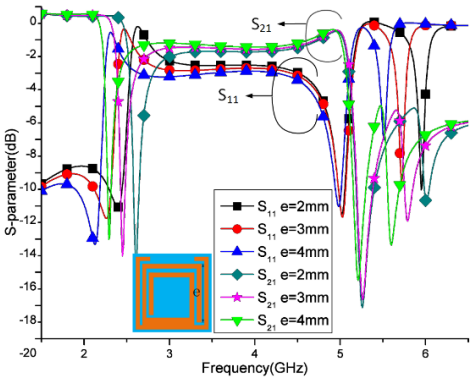

(a) Magnitude difference of the DBMC

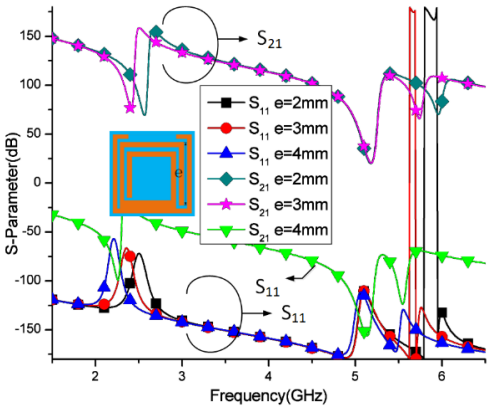

(b) Phase difference of the DBMC

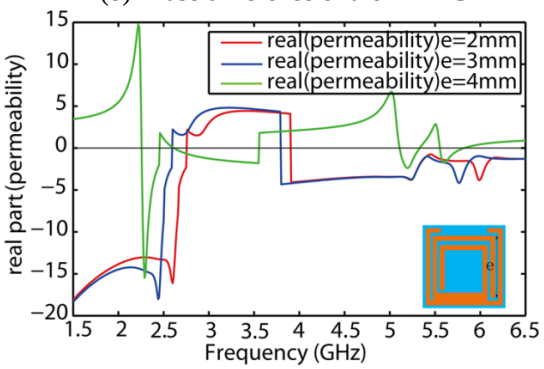

(c) Negative permittivity characteristics the DBMC

Fig. 6. Performance of the proposed DBMC with different e.

From the above discussions of the proposed DBMC, it is observed that the gap between the SRRs and the length of the SRRs decide the magnitude and phase of the transmission coefficient (S_{21}) and reflection coefficient (S_{11}) over the upper and lower operating bands of the DBMC. Then the upper and lower negative permeability bands of the proposed DBMC can be extracted from the magnitude and the phase of the S_{11} and S_{22}. Thus, the decoupling DBMC array composed of two columns of DBMC cells performs high impendence at the upper and lower negative permeability bands, which can be used to prohibit the propagation of the

electromagnetic wave between the dual-band MIMO antenna array elements. The upper permeability band can be properly also be properly adjusted, which make the negative permeability bands of the DBMC array match well with the dual-band MIMO antenna array.

III. DUAL-BAND DECOUPLING MIMO ANTENNA ARRAY BASED ON PERIODIC DBMCs

In this paper, the designed DBMC is used and periodically installed in the middle of the two antenna elements. The original dual-band MIMO antenna array is shown in Fig. 7. The MIMO array consists of two microstrip patch antennas and a common ground plane, which is printed on a FR4 substrate with a relative permittivity of 4.4 and a loss tangent of 0.02. For the rectangle-patch-antenna, dual modes are excited based on the mechanism in the Section 2 to obtain two resonance frequencies. By properly selecting the position of the feeding, TM_{10} and TM_{01} modes are excited. However, the dual-band rectangle-patch-antenna array has strong MC due to the propagation of surface waves between antenna array elements since the antenna elements are very close. The metamaterial cell has already been investigated to suppress surface waves owing to its high impendence characteristic in the negative permeability band [37]. Then, the proposed DBMC also has the ability to inhibit the surface waves in lower and upper negative permeability bands. The mutual decoupling can be realized by integrating the dual-band MIMO antenna array and the designed DBMC on a same substrate when the operating bands of the dual-band antenna array are same with the negative permeability bands of the DBMC. A decoupling array structure consists of two columns of DBMCs, which are symmetrically placed along the X-axis and Y-axis. Then, the designed decoupling array structure is set between the two patch antennas to relieve the MC. By using the proposed DBMC decoupling array structure (DBMC-DAS), a MIMO array with high isolation is achieved, whose geometry is shown in Fig. 8.

Then, the proposed MIMO array with DBMC-DAS is well optimized by the HFSS, and the finalized dimensions of the MIMO array are shown in Table 1.

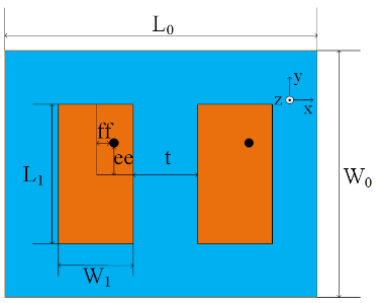

Fig. 7. Reference MIMO array.

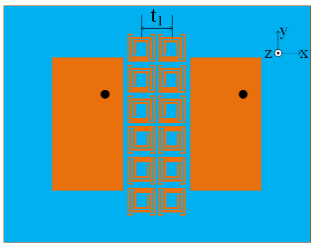

Fig. 8. Proposed MIMO array with DBMC-DAS.

Table 1: Parameters of the dual-band MIMO antenna array with high isolation (Unit: mm)

Parameters	h	W_0	ee	ff	b	g	L_0	L_1
Values	1.6	52	4.012	3.5	2.5	0.2	60	30
Parameters	e	t	t_1	a	c	s	d	W_1
Values	4	14	6	5.62	0.3	0.1	3.5	12

The optimized dual-band MIMO antenna array with proposed DBMC-DAS is fabricated, and the photograph of the fabricated MIMO array is shown in Fig. 9. Then, the fabricated MIMO antenna is measured by using Agilent N9923A in a chamber. The S_{11} and S_{21} of the MIMO array are compared in Fig. 10 for measurement and simulations. We can see that the MIMO antenna has two operating bands at the lower and upper WLAN frequencies. Additionally, the measured S_{11} meets the simulation one. The difference between the measurement and the simulation is attributed to the fabrication tolerance, the stability of the FR4 substrate and the soldering. From the coupling presented by the S_{21}, it is found that the MC between the two patch antennas is reduced by the DBMC-DAS at the expected operating bands, and its MC is reduced by 15dB and 9dB for the lower and upper operating bands, respectively. Thus, the DBMC-DAS can effectively improve the isolation between the two antenna elements. To better understand the MC reduction principle of the proposed MIMO array behind the S-parameter, the current distributions and radiation patterns are analyzed based on the HFSS, and its performance is presented in Figs. 11 and 12 respectively. From the surface current distributions of the MIMO array, we observed that the strong current distributed on both the patch antenna elements for the MIMO antenna without DBMC-DAS. In a word, there is MC effect between the two antenna elements. When the DBMC-DAS is inserted into the middle of the two antenna elements, the surface current on the adjacent patch antenna element is very small while the current on the DBMC-DAS is very strong. It is evident that the DBMC-DAS decoupling structure significantly interacts with the surface currents to block them from affecting adjacent radiation elements in the MIMO antenna array. Thus, the surface current from one antenna to another antenna is blocked by the DBMC-DAS, and hence, the isolation between the MIMO antenna elements are

improved.

Then, the radiation patterns of the MIMO antenna array are obtained in a chamber, which are shown in Fig. 12. We can see that the proposed MIMO antenna has a good radiation patterns at both 2.4GHz and 5.25GHz, which is useful for small station applications. The gains of the MIMO antenna array at the two band are 2dBi and 4.6dBi, respectively.

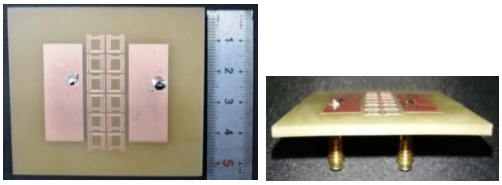

(a) Top view (b) Side view

Fig. 9. Photograph of the fabricated dual-band MIMO array.

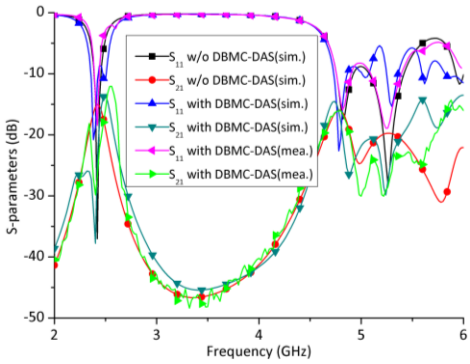

Fig. 10. S-parameter of the proposed MIMO array with DBMC-DAS.

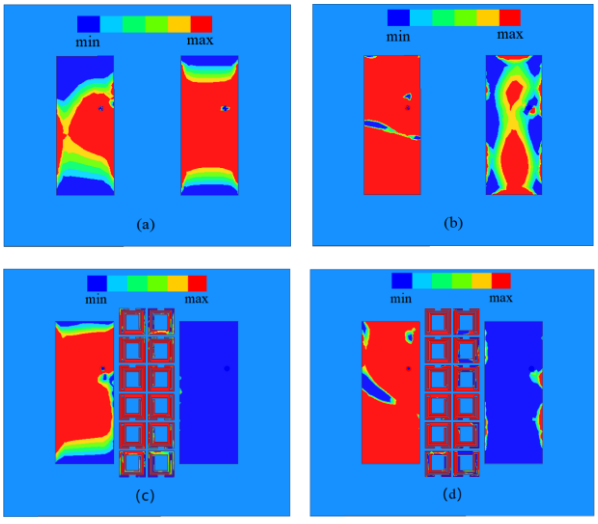

Fig. 11. Surface current distribution of the MIMO antenna: (a) 2.4GHz w/o DBMC-DAS, (b) 5.25GHz w/o DBMC-DAS, (c) 2.4GHz with DBMC-DAS, and (d) 5.25GHz with DBMC-DAS.

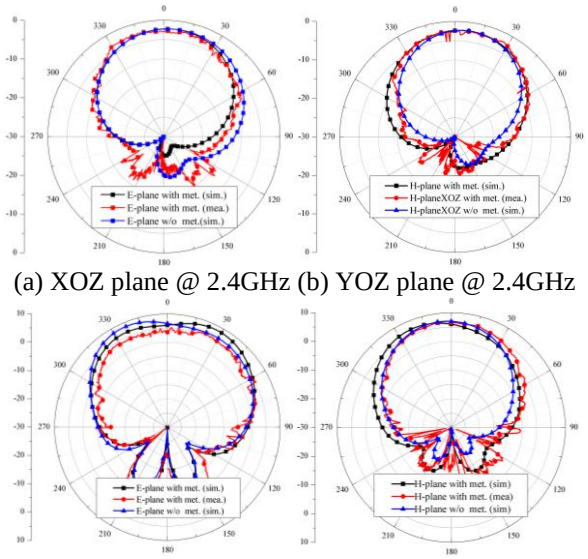

(a) XOZ plane @ 2.4GHz (b) YOZ plane @ 2.4GHz

(c) XOZ plane @ 5.25GHz (d) YOZ plane @ 5.25GHz

Fig. 12. Radiation patterns of the MIMO antenna array.

In order to show the priority of the high isolation dual-band antenna array in this paper, a comparison with the recent designs [40-44] is listed in Table 2. From the Table 2, it is found that the overall size of this high isolation antenna array is almost the smallest one, and its bandwidth covers the WLAN.

Table 2: Comparisons of proposed antennas with previous works

Refs.	10-dB BW (Low Band)	10-dB BW (High Band)	Isolation Enhancement at f_l (dB)	Isolation Enhancement at f_h (dB)	Total Size (λ_0 in GHz)
[40]	NA	NA	15.14	16.26	$1.14\lambda_{3.4}\times0.68\lambda_{3.4}$
[41]	7.4%	5.7%	6	6	$1.26\lambda_{2.7}\times0.63\lambda_{2.7}$
[28]	4.2%	3.8%	12	20	$0.88\lambda_{2.7}\times0.44\lambda_{2.7}$
[42]	9.5%	12.2%	20	8	$1.23\lambda_{1.795}\times0.42\lambda_{1.795}$
[43]	1.7%	0.75%	10.8	15.6	$0.41\lambda_{3.5}\times0.41\lambda_{3.5}$
This work	4.2%	2.3%	15.5	9	$0.48\lambda_{3.5}\times0.41\lambda_{3.5}$

IV. CONCLUSION

In this paper, a dual-band MIMO array with dual-frequency metamaterial decoupling structure is proposed and its performance is analyzed and discussed in detail. The DBMC-DAS consists of 6×2 dual-frequency metamaterial decoupling cells that are set in the middle of the two patch antenna elements. The proposed MIMO array with DBMC-DAS has been optimized, fabricated and measured. The results showed that the MC has been reduced by 15dB and 9dB for the lower and upper operating bands while the radiation patterns and the bandwidth of the MIMO array remain the same as that of the MIMO array without the DBMC-DAS. The proposed high isolation MIMO array with compact size can effectively reduce the mutual coupling without sacrificing

the radiation patterns. The advantage of the proposed technique is its simplicity and it can be easily retrofitted to existing antenna arrays quickly and at low cost.

ACKNOWLEDGMENT

This work was partially supported by the National Key Research and Development Program of China (2016YFE111100), Key Research and Development Program of Heilongjiang (GX17A016), the Science and Technology innovative Talents Foundation of Harbin (2016RAXXJ044), the Natural Science Foundation of Beijing (4182077), China Postdoctoral Science Foundation (2017M620918) and the Fundamental Research Funds for the Central University (HEUCFM180806).

REFERENCES

[1] C. A. Balanis, *Antenna Theory, Analysis and Design*. John Wiley & Sons, Inc. 1982.

[2] Y. Yang, Q. Chu, and C. Mao, "Multiband MIMO antenna for GSM, DCS, and LTE indoor application," *IEEE Antennas and Wireless Propag. Lett*., vol. 15, pp. 1573-1576, 2016.

[3] Y. Li, W. Li, and W. Yu, "A multi-band/UWB MIMO/diversity antenna with an enhance isolation using radial stub loaded resonator," *Applied Computational Electromagnetics Society Journal*, vol. 28, pp. 8-20, 2013.

[4] S. Zhang, Z. Ying, J. Xiong, and S. He, "Ultra-wideband MIMO/diversity antennas with a tree-like structure to enhance wideband isolation," *IEEE Antennas and Wireless Propag. Lett*., vol. 8, pp. 1279-1282, 2009.

[5] Y. Li, T. Jiang, and R. Mittra, "A miniaturized dual-band antenna with toothbrush-shaped patch and meander line for WLAN applications," *Wireless Personal Communications*, vol. 91, pp. 595-602, 2016.

[6] Y. Li, W. Li, and Q. Ye, "A reconfigurable triple notch band antenna integrated with defected microstrip structure band-stop filter for ultra-wideband cognitive radio applications," *International Journal of Antennas and Propagation*, vol. 2013, Article ID: 472645, pp. 1-13, 2013.

[7] J. H. Chou, J. F. Chang, D. B. Lin, and T. L. Wu, "Dual-band WLAN MIMO antenna with a decoupling element for full-metallic bottom cover tablet computer applications," *Microwave and Optical Technology Letters*, vol. 60, no. 5, pp. 1245-1251, 2018.

[8] Q. Luo, J. R. Pereira, and H. M. Salgado, "Reconfigurable dual-band C-shaped monopole antenna array with high isolation," *Electronics Letters*, vol. 46, no. 13, pp. 888-889, 2010.

[9] Y. T. Wu, Q. X. Chu, and S. J. Yao, "A dual-band printed slot diversity antenna for wireless communication terminals," *2013 IEEE International Wireless Symposium (IWS)*, Beijing, China, 2013.

[10] Q. L. Li, S. W. Cheung, D. Wu, and T. I. Yuk, "Optically transparent dual-band MIMO antenna using micro-metal mesh conductive film for WLAN system," *IEEE Antennas and Wireless Propag. Lett*., vol. 16, pp. 920-923, 2016.

[11] S. Shoaib, I. Shoaib, N. Shoaib, X. Chen, and C. Parini, "Design and performance study of a dual-element multiband printed monopole antenna array for MIMO terminals," *IEEE Antennas and Wireless Propag. Lett*., vol. 13, pp. 329-332, 2014.

[12] M. S. Khan, M. F. Shafique, A. Naqvi, et al., "A miniaturized dual-band MIMO antenna for WLAN applications," *IEEE Antennas and Wireless Propag. Lett*., vol. 14, pp. 958-961, 2015.

[13] E. Rajo-Iglesias, O. Quevedo-Teruel, and M. Sainchez-Ferflifldez, "Compact multimode patch antennas for MIMO applications," *IEEE Antennas and Propagation Magazine*, vol. 50, no. 2, pp. 197-205, 2008.

[14] T. Zhang, W. Hong, Y. Zhang, and K. Wu, "Design and analysis of SIW cavity backed dual-band antennas with a dual-mode triangular-ring slot," *IEEE Trans. Antennas Propag*., vol. 62, no. 10, pp. 5007-5016, 2014.

[15] D. K. Karmokar and K. P. Esselle,"Periodic U-slot-loaded dual-band half-width microstrip leaky-wave antennas for forward and backward beam scanning," *IEEE Trans. Antennas Propag*., vol. 63, no. 12, pp. 5372-5381, 2015.

[16] U. Chakraborty, A. Kundu, S. K. Chowdhury, and A. K. Bhattacharjee, "Compact dual-band microstrip antenna for IEEE 802.11a WLAN application," *IEEE Antennas and Wireless Propag. Lett*., vol. 13, pp. 407-410, 2014.

[17] S. Liu, W. Wu, and D. Fang, "Single-feed dual-layer dual-band E-shaped and U-slot patch antenna for wireless communication application," *IEEE Antennas and Wireless Propag. Lett*., vol. 15, pp. 468-471, 2016.

[18] Q. Luo, S. Gao, and L. Zhang, "Wideband multi-layer dual circularly polarised antenna for array application," *Electronics Letters*, vol. 51, no. 25, pp. 2087-2089, 2015.

[19] X. W. Dai, T. Zhou, and G. Cui, "Dual-band microstrip circular patch antenna with monopolar radiation pattern," *IEEE Antennas and Wireless Propag. Lett*., vol. 15, pp. 1004-1007, 2016.

[20] R. G. Vaughan and J. B. Andersen, "Antenna diversity in mobile communications," *IEEE Trans. Veh. Technol*., vol. VT-36, no. 4, pp. 149-172, Nov. 1987.

[21] M. Bouezzeddine and W. L. Schroeder, "Design of a wideband, tunable four-port MIMO antenna system with high isolation based on the theory of characteristic modes," *IEEE Trans. Antennas*

Propag., vol. 64, no. 7, pp. 2679-2688, 2016.

[22] B. Wang, Y. Chang, and Y. Sun, "Performance of the large-scale adaptive array antennas in the presence of mutual coupling," *IEEE Trans. Antennas Propag*., vol. 64, no. 6, pp. 2236-2245, June 2016.

[23] R. Janaswamy, "Effect of element mutual coupling on the capacity of fixed length linear arrays," *IEEE Antennas Wireless Propag. Lett*., vol. 1, no. 1, pp. 157-160, 2002.

[24] J. Sui and K.-L. Wu, "A general T-stub circuit for decoupling of two dual-band antennas," *IEEE Transactions on Microwave Theory and Techniques*, vol. 65, no. 6, pp. 2111-2121, 2017.

[25] C. Wu, G. Zhou, Y. Wu, and T. Ma, "Stub-loaded reactive decoupling network for two-element array using even–odd analysis," *IEEE Antennas and Wireless Propag. Lett*., vol. 12, pp. 452-455, 2013.

[26] R. Xia, S. Qu, P. Li, D. Yang, S. Yang, and Z. Nie, "Wide-angle scanning phased array using an efficient decoupling network," *IEEE Trans. Antennas Propag*., vol. 63, no. 11, pp. 5161-5165, 2015.

[27] L. Zhao and K. Wu, "A dual-band coupled resonator decoupling network for two coupled antennas," *IEEE Trans. Antennas Propag*., vol. 63, no. 7, pp. 2843-2850, 2015.

[28] L. Zhao, F. Liu, X. Shen, G. Jing, Y. Cai, and Y. Li, "A high-pass antenna interference cancellation chip for mutual coupling reduction of antennas in contiguous frequency bands," *IEEE Access*, vol. 6, pp. 38097-38105, 2018.

[29] A. Ghalib and M. S. Sharawi, "TCM analysis of defected ground structures for MIMO antenna designs in mobile terminals," *IEEE Access*, vol. 5, pp. 19680-19692, 2017.

[30] K. Wei, J. Li, L. Wang, Z. Xing, and R. Xu, "S-shaped periodic defected ground structures to reduce microstrip antenna array mutual coupling," *Electronics Letters*, vol. 52, pp. 1288-1290, 2016.

[31] K. Wei, J. Li, L. Wang, Z. Xing, and R. Xu, "Mutual coupling reduction by novel fractal defected ground structure bandgap filter," *IEEE Trans. Antennas Propag.*, vol. 64, pp. 4328-4335, 2016.

[32] F. Yang and Y. Rahmat-Samii, "Microstrip antennas integrated with electromagnetic band-gap (EBG) structures: A low mutual coupling design for array applications," *IEEE Trans. Antennas Propag*., vol. 51, pp. 2936-2946, 2003.

[33] T. Jiang, T. Jiao, and Y. Li, "Array mutual coupling reduction using L-loading E-shaped electromagnetic band gap structures," *International Journal of Antennas and Propagation*, vol. 2016, Article ID 6731014, 9 pages, 2016.

[34] T. Jiang, T. Jiao, and Y. Li, "A low mutual coupling MIMO antenna using periodic multi-layered electromagnetic band gap structures," *Applied Computational Electromagnetics Society Journal*, vol. 33, no. 3, 2018.

[35] M. S. Alam, M. T. Islam, and N. Misran, "A novel compact split ring slotted electromagnetic bandgap structure for microstrip patch antenna performance enhancement," *Progress in Electromagnetics Research*, vol. 130, pp. 389-409, 2012.

[36] H. N. B. Phuong, H. V. Phi, N. K. Kiem, and D. N. Dinh, "Design of compact EBG structure for array antenna application," *2015 International Conference on Advanced Technologies for Communications (ATC)*, Oct. 2015.

[37] M. A. Abdalla and A. A. Ibrahim, "Compact and closely spaced metamaterial MIMO antenna with high isolation for wireless applications," *IEEE Antennas and Wireless Propag. Lett*., vol. 12, pp. 1452-1455, 2013.

[38] D. A. Ketzaki and T. V. Yioultsis, "Metamaterial-based design of planar compact MIMO monopoles," *IEEE Transactions on Antennas and Propagation*, vol. 61, no. 5, pp. 2758-2766, 2013.

[39] K. Yu, Y. Li, and X. Liu, "Mutual coupling reduction of a MIMO antenna array using 3-D novel meta-material structures," *Applied Computational Electromagnetics Society Journal*, vol. 33, no. 7, pp. 758-763, 2018.

[40] B. L. Dhevi, K. S. Vishvaksenan, and K. Rajakani, "Isolation enhancement in dual-band microstrip antenna array using asymmetric loop resonator," *IEEE Antennas and Wireless Propagation Letters*, vol. 17, no. 2, pp. 238-241, 2018.

[41] G. Li, H. Zhai, Z. Ma, C. Liang, R. Yu, and S. Liu, "Isolation-improved dual-band MIMO antenna array for LTE/WiMAX mobile terminals," *IEEE Antennas and Wireless Propagation Letters*, vol. 13, pp. 1128-1131, 2014.

[42] Y. Zhang, X. Zhang, L. Ye, and Y. Pan, "Dual-band base station array using filtering antenna elements for mutual coupling suppression," *IEEE Trans. Antennas Propag*., vol. 64, no. 8, pp. 3423-3429, 2016.

[43] A. Boukarkar, X. Lin, Y. Jiang, L. Nie, P. Mei, and Y. Yu, "A miniaturized extremely close-spaced four-element dual-band MIMO antenna system with polarization and pattern diversity," *IEEE Antennas and Wireless Propagation Letters*, vol. 17, no. 1, pp. 134-137, 2018.

[44] S. Luo, Y. Li, Y. Xia, G. Yang, L. Sun, and L. Zhao, "Mutual coupling reduction of a dual-band antenna array using dual-frequency metamaterial structure," *Applied Computational Electromagnetics Society Journal*, Accepted.